International Journal of
*Molecular Sciences*

MDPI

*Article*

# Synthesis of Novel Tetra($\mu_3$-Methoxo) Bridged with [Cu(II)-O-Cd(II)] Double-Open-Cubane Cluster: XRD/HSA-Interactions, Spectral and Oxidizing Properties

**Abderrahim Titi [1,*], Mouslim Messali [1], Rachid Touzani [1], Mohammed Fettouhi [2], Abdelkader Zarrouk [3], Nabil Al-Zaqri [4], Ali Alsalme [4], Fahad A. Alharthi [4], Amjad Alsyahi [4] and Ismail Warad [5,*]**

1 Laboratory of Applied and Environmental Chemistry (LCAE), Mohammed First University, 60000 Oujda, Morocco; aboutasnim@yahoo.fr (M.M.); r.touzani@ump.ac.ma (R.T.)
2 Department of Chemistry, King Fahd University of Petroleum and Minerals, P.O. Box 5048, Dhahran 31261, Saudi Arabia; fettouhi@kfupm.edu.sa
3 Laboratory of Materials, Nanotechnology and Environment, Faculty of Sciences, Mohammed V University, Av. I bn Battouta, Box 1014, 47963 Agdal-Rabat, Morocco; azarrouk@gmail.com
4 Department of Chemistry, College of Science, King Saud University, P.O. Box 2455, Riyadh 11451, Saudi Arabia; nalzaqri@ksu.edu.sa (N.A.-Z.); aalsalme@ksu.edu.sa (A.A.); fharthi@ksu.edu.sa (F.A.A.); 438203007@student.ksu.edu.sa (A.A.)
5 Department of Chemistry, Science College, An-Najah National University, P.O. Box 7, Nablus 00970, Palestine
* Correspondence: titi_abderrahim1718@ump.ac.ma (A.T.); warad@najah.edu (I.W.)

Received: 24 October 2020; Accepted: 18 November 2020; Published: 20 November 2020


**Abstract:** A new double-open-cubane core Cd(II)-O-Cu(II) bimetallic ligand mixed cluster of type $[Cl_2Cu_4Cd_2(NNO)_6(NN)_2(NO_3)_2].CH_3CN$ was made available in $EtOH/CH_3CN$ solution. The 1-hydroxymethyl-3,5-dimethylpyrazole (NNOH) and 3,5-dimethylpyrazole (NNH) act as N,O-polydentate anion ligands in coordinating the Cu(II) and Cd(II) centers. The structure of the cluster in the solid state was proved by XRD study and confirmed in the liquid state by UV-vis analysis. The XRD result supported the construction of two octahedral and one square pyramid geometries types around the four Cu(II) centers and only octahedral geometry around Cd(II) two centers. Interestingly, NNOH ligand acts as a tetra-$\mu^3$-oxo and tri-$\mu^2$-oxo ligand; meanwhile, the N-N in NNH acts as classical bidentate anion/neutral ligands. The interactions in the lattice were detected experimentally by the XRD-packing result and computed via Hirschfeld surface analysis (HSA). The UV-vis., FT-IR and Energy Dispersive X-ray (EDX), supported the desired double-open cubane cluster composition. The oxidation potential of the desired cluster was evaluated using a 3,5-DTB-catechol 3,5-DTB-quinone as a catecholase model reaction.

**Keywords:** Cd-O-Cu cluster; XRD/HSA; catecholase; spectral

## 1. Introduction

Multinuclear cluster chemistry has gained high interest due to their biochemistry potential applications and structural diversity [1]. The synthesis of multinuclear Cu(II) complexes have been planned via various factors, for example, counter ions, ligands, reagents sequence, solvents, temperature and pH [2]. Cu(II) complexes with various ligands compositions and polynuclear structures are recorded in the literature with their molecular biology, magnetism applications and catalysis. Multi-copper clusters can enhance several oxidation reactions of amines and alcohols [3–7]. Copper (II)

complexes clusters can also serve as metallo-pharmaceutical agents as antitumor, antimicrobials, antibacterial, antifungal, antipyretic, antidiabetic and antiviral agents [8–12]. The use of O, N, P-ligands as polydentate was been a good preference to build multilateral and multinuclear architectures cluster because of their electronic, steric effect and several coordination modes [13–16]. Tetra-nuclear Cu(II) clusters are existing as hot-urge points in bioinorganic modeling, magnetochemistry, multielectron transfer and catalysis. In the two last decades, plenty of cubane clusters were prepared by using alkoxo-bridged NOO or NNO types of donor ligands were prepared until now [17–22].

On the other hand, clusters with multiple spin molecular centers revealed a good catalytic aspect, especially in industrial oxidation processes [23–29]. Clusters with chelate mixed alcoholic pyrazole ligands and metal have recently received less interest due to their difficulty in preparation, low stability and rear in collecting suitable crystals to be judged by XRD single structure analysis [25–28].

We recently synthesized several novel tetra-nuclear metal cubane clusters; their structures were evaluated by XRD analysis, and their cluster catecholase catalytic activities were also evaluated by converting catechol to O-quinone as an oxidation model [21,22,30]. In this piece of work, the bimetallic Cd-O-Cu double-open cubane $[Cl_2Cu_4Cd_2(NNO)_6(NN)_2(NO_3)_2].CH_3CN$ cluster made available using chelate NNOH and NNH ligands, the structure of the cluster was proven by XRD, the tetrahedral-$\mu_3$-O and trigonal pyramidal-$\mu_2$-O bridges were detected. The octahedral and square pyramid geometries were resolved for both the metal centers. Moreover, physicochemical and HS analyses were determined to ensure the catecholase catalytic process of the desired cluster in mild or harsh conditions.

## 2. Results and Discussion

### 2.1. Cluster Preparation

The desired bimetallic cluster was prepared by stirring $CuCl_2.2H_2O$ and $Cd(NO_3)_2.4H_2O$ metallic salts together with 1-hydroxymethyl-3,5-dimethylpyrazole (NNOH) and 3,5-dimethylpyrazole (NNH) at RT for 24 h using EtOH:$CH_3CN$ solution (Scheme 1). The desired reaction of clusterization was performed at RT in an open $O_2$ atmosphere with equivalent amounts of each ligand and metal salt, and the final bimetallic $[Cl_2Cu_4Cd_2(NNO)_6(NN)_2(NO_3)_2].CH_3CN$ cluster was isolated in 78% yield. Moreover, the 3D structure was definite by XRD analysis (for the first time).

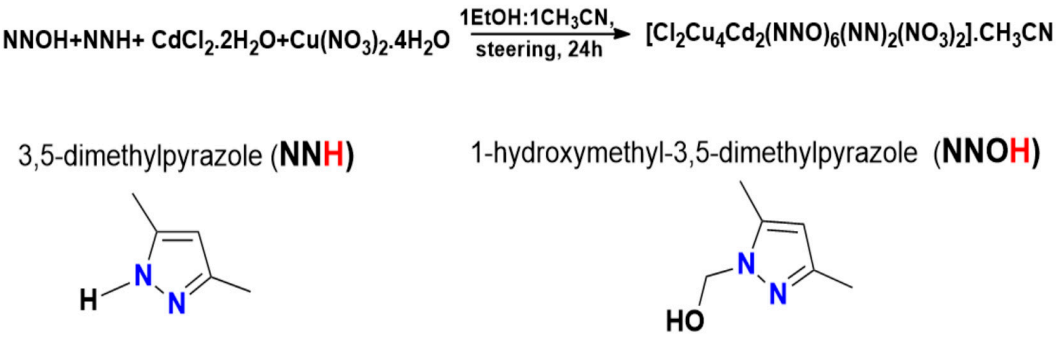


**Scheme 1.** Synthesis of the $[Cl_2Cu_4Cd_2(NNO)_6(NN)_2(NO_3)_2].CH_3CN$ bimetallic cluster.

### 2.2. Single Crystal X-ray Diffraction (SC-XRD) Investigation

The 3D structure of the newly desired cluster is shown in Figure 1, whereas the selected atomic and angles distances are provided in Table 1. The cluster crystallized in the monoclinic/*P*21/*c* crystal system and space group, respectively. The cluster crystalized with 4Cu and 2Cd metal ion double open cubane core centers with $[Cl_2Cu_4Cd_2(NNO)_6(NN)_2(NO_3)_2].CH_3CN$ formula. All the organic NNOH and NNH and inorganic $NO_3$ and Cl ligands acted as chelate or bridge anion donors, which stabilized the cluster as neutral with no, counter ions (Figure 1a). No solvents like MeOH or water molecules were detected, but only one uncoordinated $CH_3CN$ molecule was present in the crystal lattice (Figure 1b). The cationic units of the two Cd(II) and four Cu(II) centers were not directly bonded. On the other hand,

all the centers had methoxo-bridge like $4\mu^3$-O, $2\mu^2$-O, $2\mu^2$-$NO_3$ or $2\mu^2$-Cl- bridge functional groups. Furthermore, both $NN^-$ ligands, which acted as terminal bridge donors bidentate that coordinated to the Cu(II) centers only, supported the formation of two different Cu(II) geometrical centers: terminal 2Cu(II) centers with 6-coordinate [2N, 3O, 1Cl], constructing an octahedral center. Both centers were saturated with one O∩O-bidentate $NO_3$ ligand (Figure 1c). Conversely, the other Cu(II) core centers were sterically forced to be with 5-coordinate [2N, 3O], constructing a square pyramid geometry center with $\tau_{[1O2O6N1N]}$ = 3.12 °C (Figure 1d). Both core 2Cd(II) centers were constructed with distorted octahedral centers once the 6-coordinates [1N, 4O, 1Cl] were recorded (Figure 1e). It was delightful to observe that $NNO^-$ ligands coordinated with the both Cu and Cd centers via $\eta^3$:$\eta^1$-O,N-modes of coordination, hence the di-$\mu^2$-methoxo-trigonal pyramid-O center (Figure 1f), and two different tetra-$\mu^3$-methoxo-tetrahedral-O centers (Figure 1g,h).

**Table 1.** Selected bond (Å) and angles lengths (°) of the desired cluster.

| No. | Bond Type | | Bond Length Å | No. | Angle Type | | | Angle Value (°) |
|---|---|---|---|---|---|---|---|---|
| 1 | Cu2 | N1 | 1.972 (5) | 1 | N2 | Cu1 | N8 | 170.5 (2) |
| 2 | Cu1 | N2 | 1.951 (6) | 2 | N2 | Cu1 | O3 | 94.5 (2) |
| 3 | Cu1 | O3 | 2.030 (4) | 3 | N2 | Cu1 | O4 | 93.7 (2) |
| 4 | Cu1 | O4 | 2.041 (6) | 4 | N2 | Cu1 | O5 | 92.8 (2) |
| 5 | Cu1 | O5 | 2.662 (8) | 5 | N2 | Cu1 | Cl1 | 96.3 (2) |
| 6 | Cu1 | Cl1 | 2.712 (3) | 6 | N8 | Cu1 | O3 | 80.1 (2) |
| 7 | Cu2 | O1 | 2.008 (4) | 7 | N8 | Cu1 | O4 | 89.3 (2) |
| 8 | Cu2 | N6 | 2.010 (5) | 8 | N8 | Cu1 | O5 | 81.9 (2) |
| 2 | Cu1 | N8 | 1.995 (6) | 9 | N8 | Cu1 | Cl1 | 91.5 (2) |
| 10 | Cu2 | O2 | 1.927 (4) | 10 | O3 | Cu1 | O4 | 161.0 (2) |
| 11 | Cu2 | O3 | 2.279 (5) | 11 | O3 | Cu1 | O5 | 110.5 (2) |
| 12 | Cd1 | Cl1 | 2.542 (3) | 12 | O3 | Cu1 | Cl1 | 89.2 (1) |
| 13 | Cd1 | N4 | 2.301 (5) | 13 | O4 | Cu1 | O5 | 51.9 (2) |
| 14 | Cd1 | O1 | 2.472 (4) | 14 | O4 | Cu1 | Cl1 | 106.9 (2) |
| 15 | Cd1 | O2 | 2.235 (5) | 15 | O5 | Cu1 | Cl1 | 157.5 (2) |
| 16 | Cd1 | O1 | 2.299 (5) | 16 | N1 | Cu2 | N6 | 101.6 (2) |
| 17 | Cd1 | O3 | 2.362 (4) | 17 | N1 | Cu2 | O1 | 93.2 (2) |
| 18 | Cl1 | Cu1 | 2.712 (3) | 18 | N1 | Cu2 | O2 | 167.2 (2) |
| 19 | N1 | N2 | 1.395 (9) | 19 | N1 | Cu2 | O3 | 90.6 (2) |

Experimentally, several polar shorter interactions < 3 Å were detected in the crystal lattice since the cluster contains O, N and Cl heteroatoms together with polar H atoms. The non-bonded O atom of $NO_3$ ligands played a critical role in the building of the net of H-bonds in cluster lattice. Therefore, $4 \times 2$ $H_{CH}$ . . . .$O\text{-}_{NO2}$ with 2.58 and 2.70 Å (Figure 2a) with full geometric parameters (Å, degree) are illustrated in Table 2 are recorded. The C-H . . . ..πC=C ring of NN ligands as a short interaction with 2.80 Å distance played a critical role in stabilizing the crystal lattice since four bonds of such type were recorded (Figure 2b) and the interesting solvent interactions 2Cl . . . . Π $CN_{CH3CN}$ with 3.56 Å (Figure 2c) [31–35].

**Table 2.** Geometric parameters (Å, degree) for C-H . . . O interactions.

| D-H | d(D-H) | d(H..A) | <DHA | d(D..A) | A |
|---|---|---|---|---|---|
| C6-H6A | 0.970 | 2.620 | 127.17 | 3.298 | O2 [i] |
| C18-H18A | 0.970 | 2.578 | 141.13 | 3.388 | O6 [ii] |

Symmetry code: i: −x + 1, −y + 1, −z + 1; ii: −x + 1, −y + 1, −z + 1.

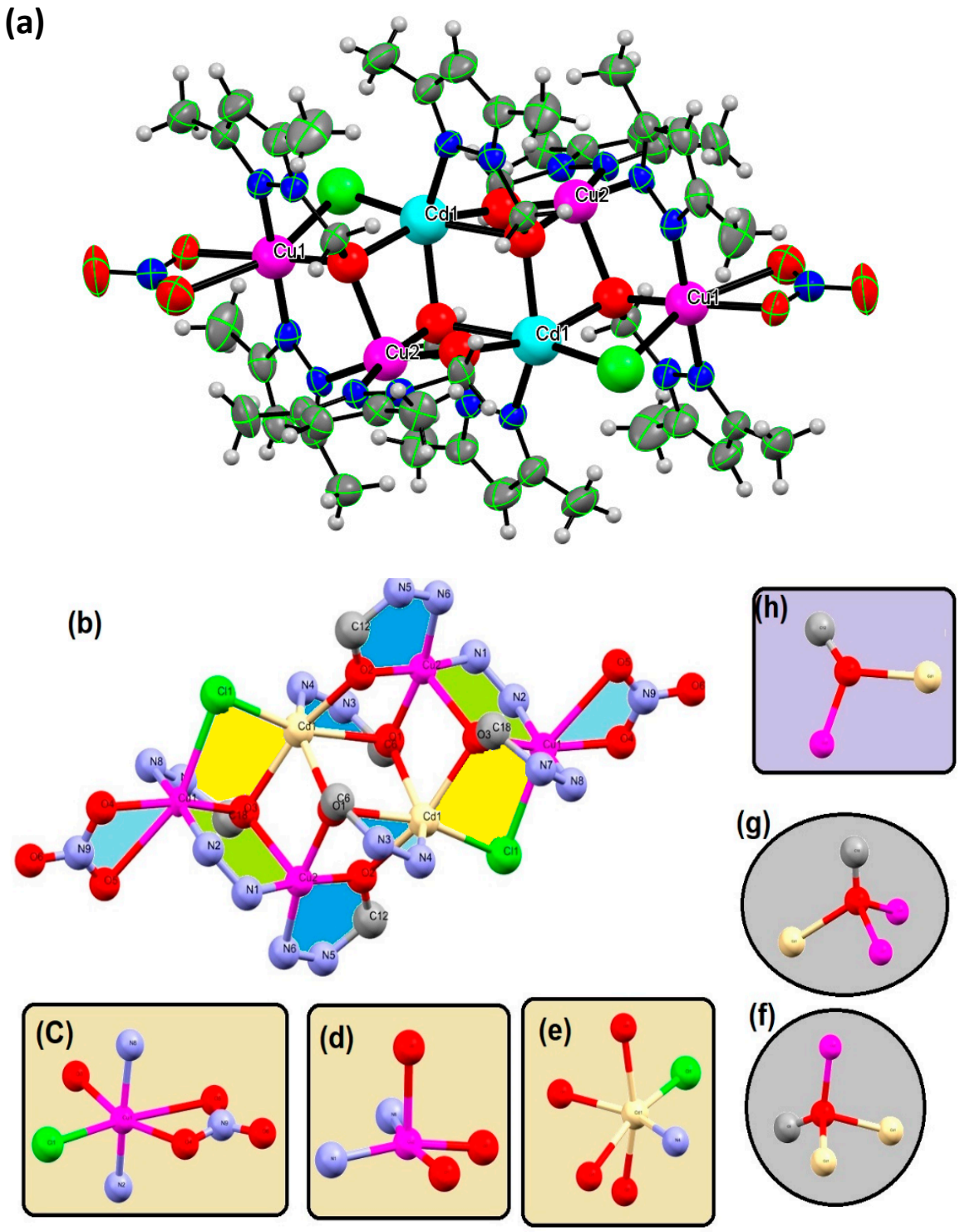


**Figure 1.** (**a**) ORTEP structure (50% probability) of the bimetallic cluster, (**b**) molecular structure without protons showing no water in the crystal lattice, (**c**) octahedral geometry around Cu(II) centers, (**d**) pyramid geometry around the other Cu(II) centers, (**e**) distorted octahedral geometry around Cd(II) centers, (**f**) di-$\mu^2$-methoxo-trigonal pyramid-O centers, (**g**) and (**h**) two different tertra-$\mu^3$-methoxo-tetrahedral-O centers.

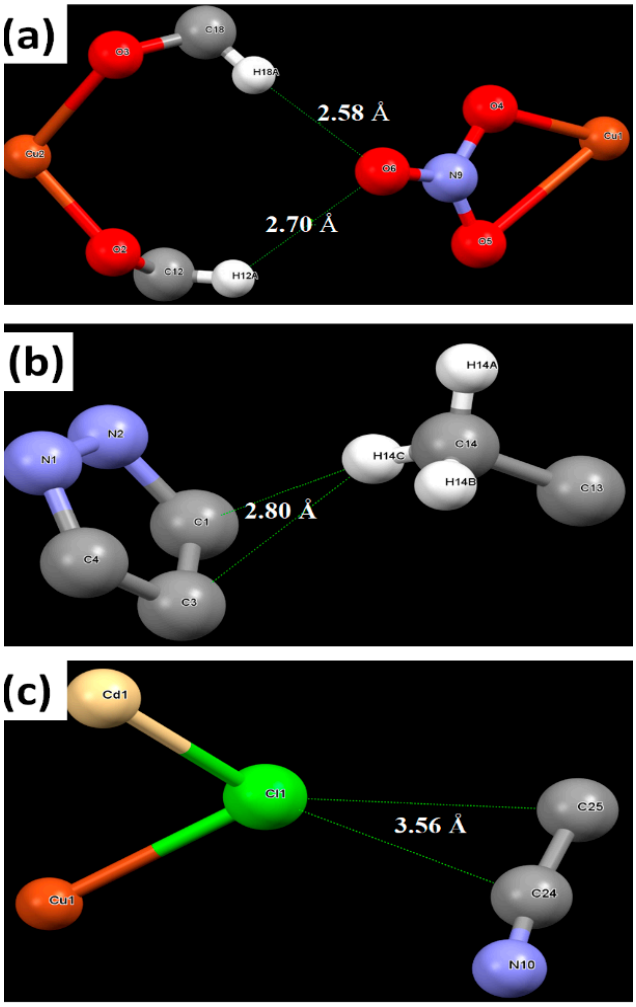


**Figure 2.** (**a**) H . . . .O-$NO_2$ H-bonds, (**b**) H . . . ΠC=C and (**c**) Cl . . . . ΠC$N_{CH3CN}$ interactions.

### *2.3. HS and 2D-FP Investigation*

The surface was mapped to obtain more interaction information on the molecule and its surrounding molecules in the crystal lattice that played critical roles in stabilizing the structural formula via short intermolecular forces reflected by red spot sizes on the normalized $d_{norm}$ [36–41]. The results illustrated in Figure 3 showed that the values of HS with three-dimensional shape and cave centers and shape ranged from 0.723 to 1.874 a.u. The red spots were behind the polar atoms such as oxygen, nitrogen, chlorine and hydrogen. Eleven red points were detected on the computed cluster surface, and they were attributed to the existence of 8 H-bond interactions. Two C-H . . . ..O-$NO_2$ (Figure 3a–c) formed H-bonds with a distance of 2.56 and 2.72 Å and two $C_{ring}$-H . . . .C=C with a length of 2.76 Å (Figure 3d). The computed HS and experimental XRD interactions were highly matched in their positions and structural parameter values.

The 2D-FP plots illustrated in Figure 4 were constructed from the 2D-HS by considering outside and inside closest-neighbor molecules. These integrated visions on contacts were helpful in the imagining of nonpolar and polar atoms interactions contributions in the cluster lattice. The other atom . . . atom contact rations were resolved as H . . . H (60.0%). Intermolecular contacts showed the larger contribution part and H . . . ..M (Cu and Cd) (0.0%) interactions ratio. Early studies concerned H . . . H connections as steric repulsive interactions that disturb the molecular system [42]. Moreover, the understanding of H . . . H interactions was verified and changed in the 1990s since a new type of interaction named the dihydrogen bond (DHB) was recorded in crystal structures of different organometallic complexes [42–45]. The other atom . . . atom intermolecular forces are illustrated in the

following importance order: H . . . .H (60.0%) > H . . . .C(10.0%) >H . . . .N (5.6%) >H . . . ..O (5.40%) > H . . . ..Cl(1.0%) >H . . . .M(0.0%).

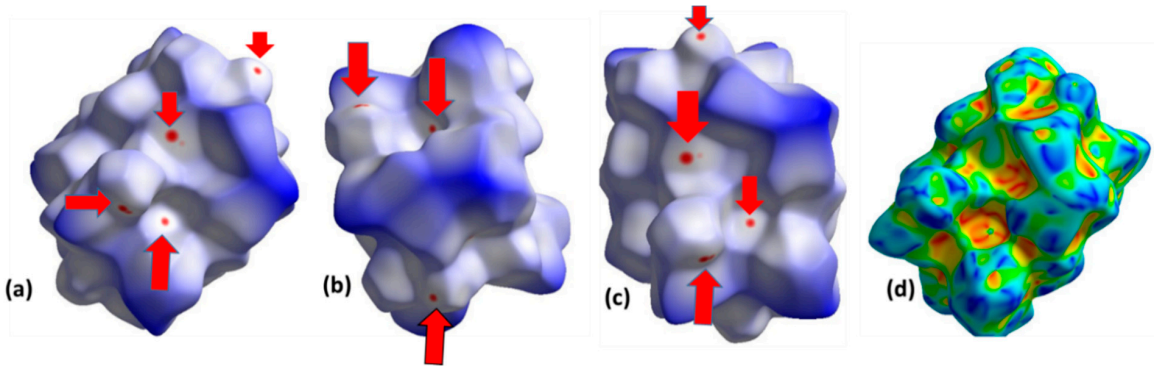


**Figure 3.** HSA-mapped (**a**–**c**) $d_{norm}$ and (**d**) shape index.

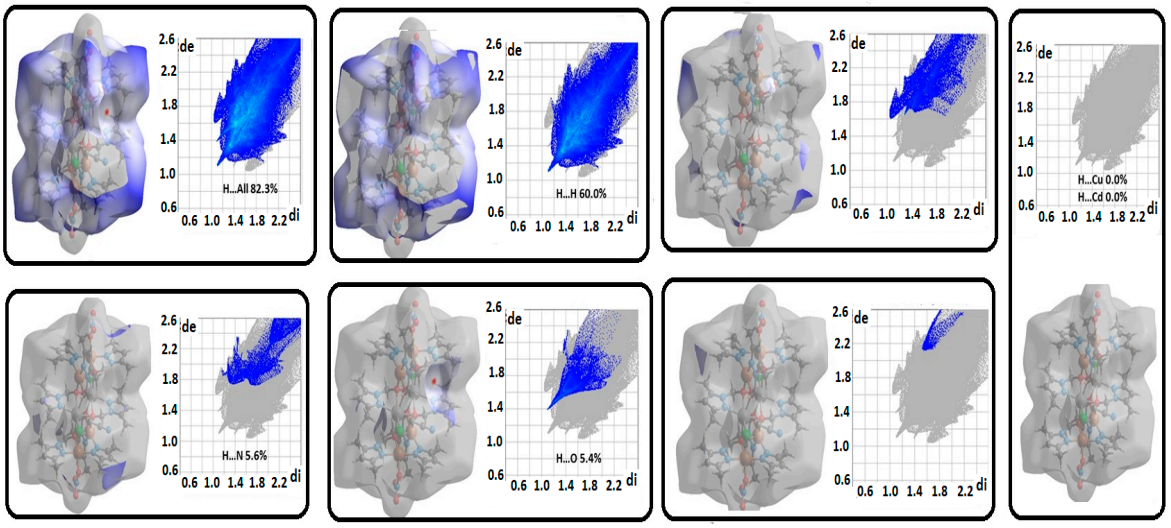


**Figure 4.** HSA-computed cluster structure together with 2D-FP and H . . . .X% interaction ratios.

### *2.4. FT-IR and EDX Investigations*

For the preparation of $[Cl_2Cu_4Cd_2(NNO)_6(NN)_2(NO_3)_2]$, the $CH_3CN$ cluster was followed up by FT-IR, as shown in Figure 5. The obtained bimetallic cluster reflected several IR bands matching with its continent functional groups. Several stretching vibrations were exposed in the cluster backbone like aliphatic and aromatic C-H, $NO_3$, C=N, MeCN, C-O, C=C, Cu-O, Cd-O, Cu-N, Cd-N and M-Cl, which were cited to their expected wavenumbers (see experimental part). Kinetically, the important changes supporting the clusterization process were the vanishing of N-H (in NNH ligand) peak at 3170 $cm^{-1}$ by the complexation NNH with metal centers and the appearing of new M-O/M-N bands at >400 $cm^{-1}$ chemical shifts [21,22]. The broad peak at ~3400 $cm^{-1}$ was mostly due to humidity on the crystal surface of the cluster. Peaks at ~2930–2820 $cm^{-1}$ in both the ligand and the cluster were attributed to C-H stretching vibrations, the C=N stretching vibration in the free ligand shifted from 1610 $cm^{-1}$ to 1560 $cm^{-1}$ upon coordination to the metal center. The appearance of broad peaks at 265–2500 $cm^{-1}$ in the cluster was only due to the presence of MeCN stretching vibration. The C=C and C-O stretching vibrations in both ligand and cluster were the same, with ~1480 and 1100 $cm^{-1}$, respectively. The M-O and M-N bonds for the both metals (Cu and Cd) vibrations were in the low range ~400–450 $cm^{-1}$.

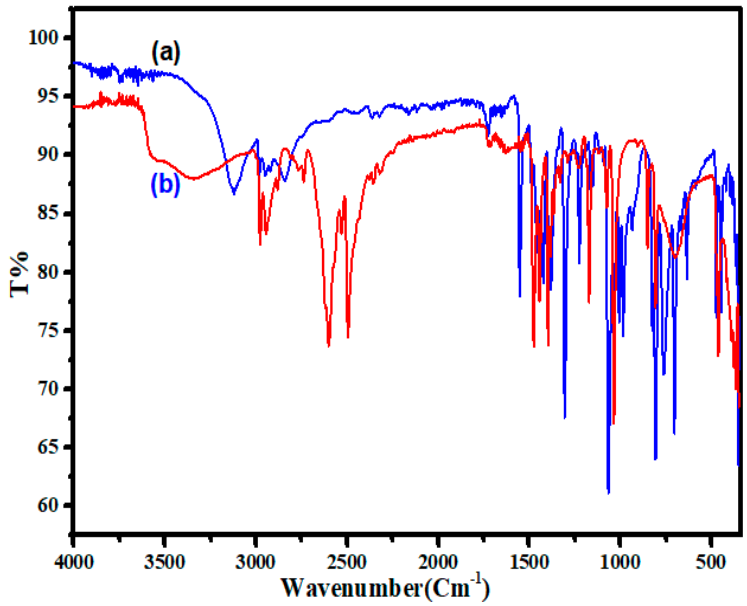


**Figure 5.** FT-IR of (**a**) 3,5-dimethylpyrazole (NNH) ligand and (**b**) the desired cluster.

The qualitative compositions of the cluster were confirmed by EDX analysis, as presented in Figure 6. The presence of Cu atoms was confirmed by energy signals at 1.2, 8.2 and 9.1 keV. Meanwhile, the Cd atoms peaks were cited to 3.3 and 3.5 keV positions, moreover, Cl to 2.4 keV position, respectively. Moreover, C, N and O atoms were cited to their expected atomic energy peaks as seen in Figure 6.

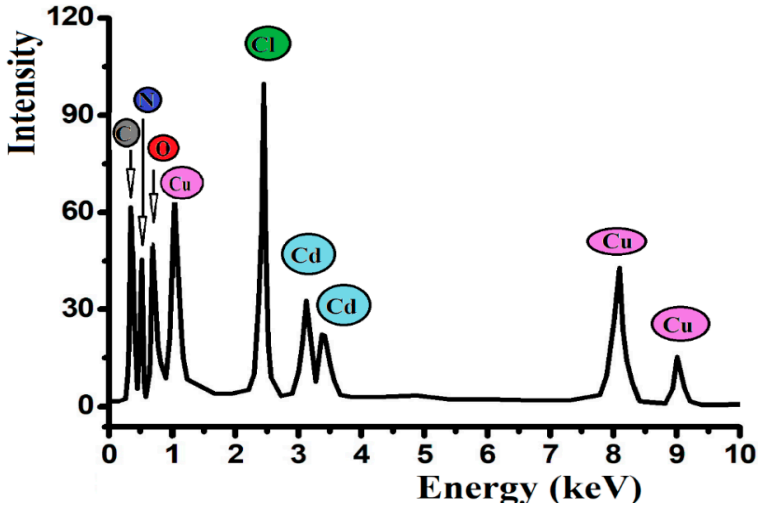


**Figure 6.** EDX spectra of the desired cluster.

*2.5. Electronic Transfer and Optical Energy Gap*

The electronic absorption of the novel desired cluster and its free ligands in DMSO solvent were combined, as illustrated in Figure 7a. Peaks in the UV-region: the recorded $\lambda_{max}$ = 280 nm ($\varepsilon = 1.0 \times 10^3$ L mol$^{-1}$ cm$^{-1}$) for the cluster, $\lambda_{max}$ = 282 nm ($\varepsilon = 1.8 \times 10^3$ L mol$^{-1}$ cm$^{-1}$) for NNH ligand and $\lambda_{max}$ = 286 nm ($\varepsilon = 1.6 \times 10^3$ L mol$^{-1}$ cm$^{-1}$) for NNOH ligand all can be assigned to $\pi \rightarrow \pi^*$ ligands e-transition. The two broad and low-intensity peaks in the visible region at $\lambda_{max}$ = 605 nm ($\varepsilon = 2.2 \times 10^2$ L mol$^{-1}$ cm$^{-1}$) and $\lambda_{max}$ = 685 nm ($\varepsilon = 8.4 \times 10^2$ L mol$^{-1}$ cm$^{-1}$) cited to the Cu(II) d-d e-transfer in the cluster only confirmed the N-M and O-M bond coordination [46]. The experimental optical band gap energies ($\Delta E_g$) in DMSO were obtained by using the Tauc relation [40]. The organic ligands direct $\Delta E_g$ was found to be 4.18 eV, as seen in Figure 7b. Meanwhile, the metallic direct $\Delta$Eg

was found to be 1.73 eV, as seen in Figure 7c. The attained $\Delta E_g$ results reflected the 4Cu(II) cluster centers complexes within the visible region; meanwhile, the NNO and NN ligands with invisible region electron transfer. Therefore, clusters with such optical performance properties are expected to be an important material for solar cells, optoelectronic devices and photonic devices [47].

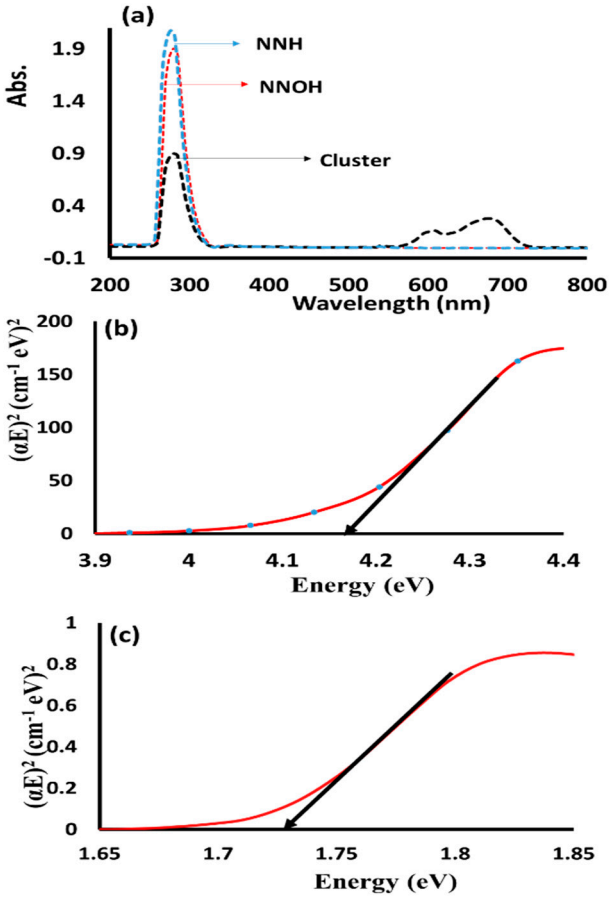


**Figure 7.** (**a**) Electronic spectra of NNH, NNOH and cluster, (**b**) optical band gap of ligands, and (**c**) optical band gap of the metal center in the cluster dissolved in DMSO.

### *2.6. Cluster Oxidation Potential toward Catecholase of Catechol*

One of the goals of the present study is to evaluate the aerobic catecholase catalytic oxidation founding of the cluster. To accomplish this, 0.1 M of 3,5-di-tert-butylbenzene-1,2-diol (3,5-DBT) was mixed with $1 \times 10^{-4}$ M of the desired cluster in DMF solvent under stirring an open RT system for around 1 h (Scheme 2). The formation of the 3,5-di-tert-butylcyclohexa-3,5-diene-1,2-dione (3,5-DTBQ) product was monitored by UV-vis analysis in 250–500 nm range [20,21,44], as seen in Figure 8.

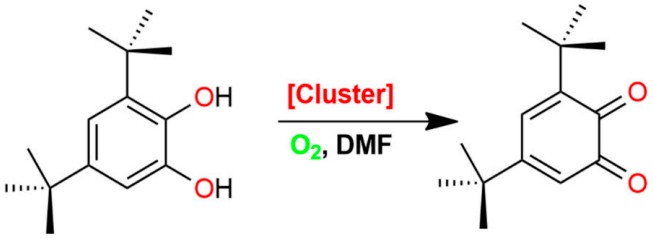


**Scheme 2.** Cluster catalytic oxidation of catechol to O-quinone.

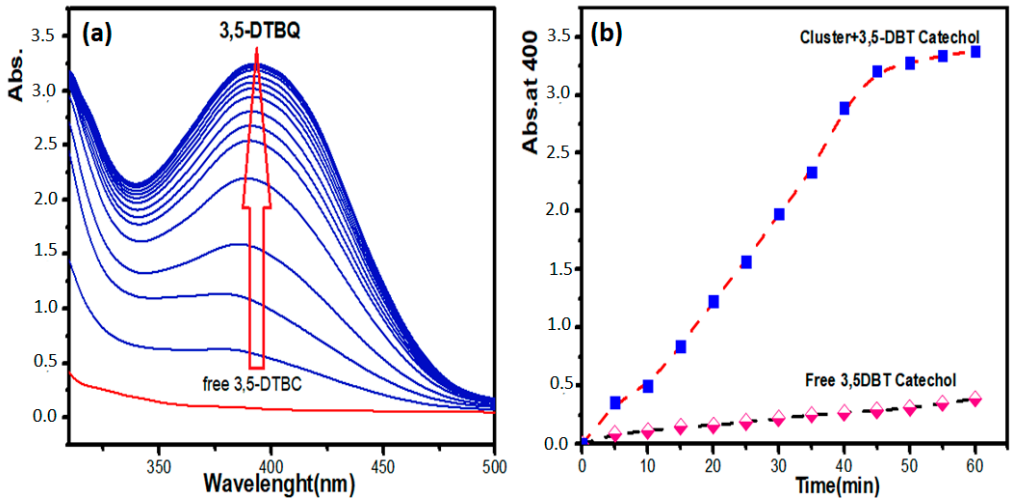


**Figure 8.** Time-dependent 3.5-DBT oxidation process: (**a**) abs. vs. λ, and (**b**) abs. vs. *t*.

In Figure 8a, the absorptions of 3,5-DTBQ product at $\lambda_{max}$~400 nm were gradually raised by time only with the presence of the cluster catalyst. The result revealed without ambiguity that the cluster acts as an excellent oxidation catalyst since the reaction was completely finished within 1 h. Moreover, neither side products nor products were detected by the UV-vis absorption in the absence of the cluster Figure 8b.

The oxidation rates of the cluster using several concentrations of 3,5-DBT find to be suited to the Michaelis–Menten plot (Figure 9a), which was linearized to Lineweaver–Burk plot (Figure 9b), in order to figure out the Vmax, KM and Kcat kinetic parameters. The kinetic parameter values were compared to similar catalytic processes [48–54]. In general, the cluster catalyst results were excellent compared to other complexes, where many factors like solvents, substrate and complex nature control the ability of catalysts [2,20,51].

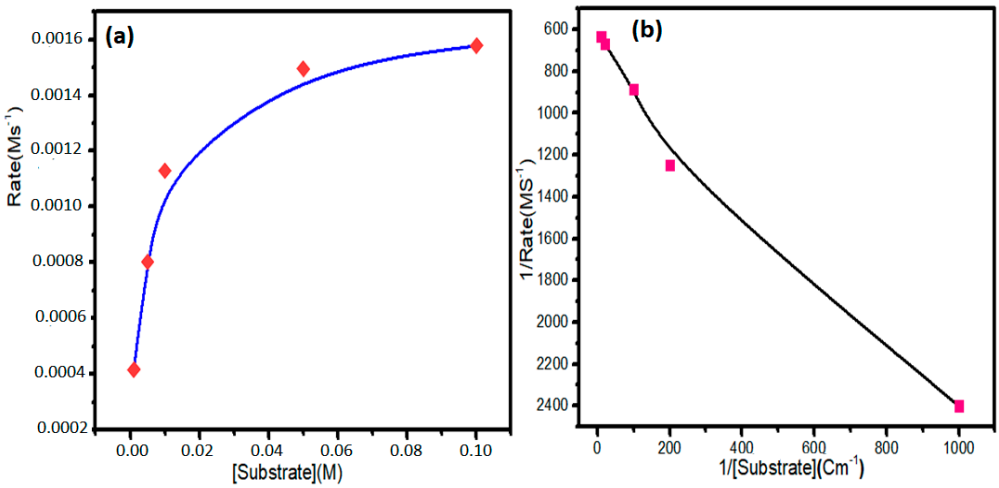


**Figure 9.** (**a**) Oxidation reaction initial rates vs. 3,5-DBT conc., and (**b**) the Lineweaver–Burk plots.

## 3. Materials and Methods

The commercially available $CdCl_2.4H_2O$ and $Cu(NO_3)_2.6H_2O$ salts, solvents and chemicals, were served without purification. The NNOH and NNH were prepared in our lab [22]. EDX was performed using Brucker D/MAX 2500 X-ray diffractometer, with λ = 1.54 Å Cu K radiation, TU-1901 double-beam UV-visible spectrophotometer was used to measure the UV-vis. The TG was carried out using TGA SDT-Q600, FT-IR spectra were performed in the range of 4000–400 cm$^{-1}$ of frequency

using a PerkinElmer Spectrum, and HS calculation was performed using CRYSTAL EXPLORER 3.1 package [33].

### *3.1. Synthesis of $[Cl_2Cu_4Cd_2(NNO)_6(NN)_2(NO_3)_2].CH_3CN$ Bimetallic Cluster*

0.16 mmol of each salt $CdCl_2.4H_2O$ and $Cu(NO_3)_2.6H_2O$ were dissolved in 50 mL of ethanol solvent. After complete dissolving, 0.16 mmol of NNOH and NNH each (in 20 mL of $CH_3CN$) were added to the reaction mixture, which was stirred for 24 h in an open condition. The reaction was then stopped and subjected to the solvent-evaporation process. After 3 weeks, light green plate crystals of $[Cl_2Cu_4Cd_2(NNO)_6(NN)_2(NO_3)_2].CH_3CN$ cluster had formed in 74% yield. Peaks of selected IR vibrations are listed as ν = 3018 (C-H), (1520–1380) ($NO_3$), 2936 (C-H), 1622 (C=N), (2200–2550) (-CN), 1485 (C=C), 1020 (C-O), $cm^{-1}$. The peak at 420–550 $cm^{-1}$ belongs to M–O and M–N stretching vibrations [21,22]. UV-vis. (DMSO) at $\lambda_{max}$ = 280, 605 and 685 nm and m.p. > 340 °C.

### *3.2. Catechol Oxidation Reaction*

The catalytic part was performed using the procedure described recently in the literature [22].

### *3.3. X-Ray*

Single crystal X-ray data were collected on a Bruker D8 Quest diffractometer (MoKα radiation λ = 0.71073 Å) at 298 K. The structure was solved by direct methods and refined by full-matrix least-squares methods based on $F^2$ using the SHELXL software [34]. Crystal data for the desired cluster is illustrated in Table 3.

**Table 3.** Crystal data and structure refinement of the desired cluster.

| **Empirical Formula** | **$C_{48}$ $H_{71}$ $Cd_2$ $Cl_2$ $Cu_4$ $N_{19}$ $O_{12}$** |
|---|---|
| Formula weight | 1656.09 |
| CCDC | 1956507 |
| Temperature | 298(2) K |
| Wavelength | 0.71073 Å |
| Crystal system | Monoclinic |
| Space group | P $2_1$/c |
| Unit cell dimensions | a = 10.860(9) Å |
| | b = 20.665(19) Å |
| | c = 17.212(16) Å |
| | B = 95.96(3)° |
| Volume | 3842(6) $Å^3$ |
| Z | 2 |
| Density (calculated) | 1.432 $g/cm^3$ |
| Absorption coefficient | 1.759 $mm^{-1}$ |
| F(000) | 1668 |
| Crystal size | 0.220 × 0.180 × 0.060 $mm^3$ |
| Theta range for data collection | 2.576 to 29.850°. |
| Index ranges | −14 ≤ h ≤ 14, −27 ≤ k ≤ 27, −23 ≤ L ≤ 24 |
| Reflections collected | 107,448 |
| Independent reflections | 9719 [R(int) = 0.0711] |
| Refinement method | Full-matrix least-squares on $F^2$ |

**Table 3.** *Cont.*

| Empirical Formula | $C_{48}$ $H_{71}$ $Cd_2$ $Cl_2$ $Cu_4$ $N_{19}$ $O_{12}$ |
|---|---|
| Data/restraints/parameters | 9719/2/401 |
| Goodness-of-fit on F2 | 1.111 |
| Final R indices [I>2sigma(I)] | R1 = 0.0719, wR2 = 0.2085 |
| R indices (all data) | R1 = 0.1029, wR2 = 0.2370 |
| Largest diff. peak and hole | 1.825 and −1.000 e.Å$^{-3}$ |

## 4. Conclusions

A new $[Cl_2Cu_4Cd_2(NNO)_6(NN)_2(NO_3)_2].CH_3CN$ cluster of type double-open cubane core with Cd(II)-O-Cu(II) center was made available. The 3D structure of the newly synthesized cluster was proven by XRD crystal. The XRD showed the presence of both octahedral and square pyramid metal ions geometry centers. Moreover, the di-$\mu^2$-methoxo-trigonal pyramid-O center and tetra-$\mu^3$-methoxo-tetrahedral-O centers were recorded. Several shot interactions like $H_{CH}$ . . . .O-$_{NO2}$, C-H . . . .$\pi$ C=$C_{NN}$ and Cl . . . . $\Pi$ CN were detected in the lattice by XRD and computed via HS-analysis. Furthermore, the cluster composition and structural behavior were proved spectrally furthermore via FT-IR, EDX and UV-vis. Finally, the cluster recorded an excellent catecholase potential when it was applied to the Catechol O-quinone room condition oxidation reaction.

**Author Contributions:** A.T. and M.M. carried out the experiments. I.W. wrote the manuscript, F.A.A., A.A. (Amjad Alsyahi) carried out the theoretical calculations. M.F. carried out XRD measurement. A.Z. and N.A.-Z. contributed to the final version of the manuscript. R.T., A.A. (Ali Alsalme) and N.A.-Z. supervised the project. All authors have read and agreed to the published version of the manuscript.

**Funding:** The authors extend their appreciation to the Deputyship for Research & Innovation, "Ministry of Education" in Saudi Arabia for funding this research work through the project number IFKSURG-1440-141.

**Conflicts of Interest:** The authors declare no competing interests.

## References

1. Paula, A.; Mistria, S.; Bertolasib, V.; Manna, S.C. DNA/protein binding and molecular docking studies of two tetranuclear Cu (II) complexes with double-open-cubane core like structure. *Inorg. Chim. Acta* **2019**, *495*, 119005. [CrossRef]
2. Zheng, S.-R.; Pan, M.; Wu, K.; Chen, L.; Jiang, J.-J.; Wang, D.-W.; Shi, J.-Y.; Su, C.-Y. Assembly of Binuclear, Tetranuclear, and Multinuclear Complexes from Pincer-Like Mononuclear Metallotectons: Structural Diversity Dependent on Precursors. *Cryst. Growth Des.* **2015**, *15*, 625–634. [CrossRef]
3. Aronica, C.; Chumakov, Y.; Jeanneau, E.; Luneau, D.; Neugebauer, P.; Barra, A.-L.; Gillon, B.; Goujon, A.; Cousson, A.; Tercero, J.; et al. Structure, Magnetic Properties, Polarized Neutron Diffraction, and Theoretical Study of a Copper(II) Cubane. *Chem. Eur. J.* **2008**, *14*, 9540. [CrossRef] [PubMed]
4. Than, R.; Feldmann, A.A.; Krebs, B. Structural and functional studies on model compounds of purple acid phosphatases and catechol oxidases.Coord. *Chem. Rev.* **1999**, *182*, 211.
5. Allen, S.E.; Walvoord, R.R.; Padilla-Salinas, R.; Kozlowski, M.C. Aerobic Copper-Catalyzed Organic Reactions. *Chem. Rev.* **2013**, *113*, 6234. [CrossRef]
6. Bilyachenko, A.N.; Dronova, M.S.; Yalymov, A.I.; Lamaty, F.; Bantreil, X.; Martinez, J.; Bizet, C.; Shul'pina, L.S.; Korlyukov, A.A.; Arkhipov, D.E.; et al. Cage-like Copper(II) Silsesquioxanes: Transmetalation Reactions and Structural, Quantum Chemical, and Catalytic Studies. *Chem. Eur. J.* **2015**, *21*, 8758. [CrossRef]
7. Dias, S.S.P.; Kirillova, M.V.; Andre, V.; Kłak, J.; Kirillov, A.M. New tricopper(II) cores self-assembled from aminoalcohol biobuffers and homophthalic acid: Synthesis, structural and topological features, magnetic properties and mild catalytic oxidation of cyclic and linear C5–C8 alkanes. *Inorg. Chem. Front.* **2015**, *2*, 525. [CrossRef]

8. Fernandes, T.A.; Santos, C.I.M.; Andre, V.; Kłak, J.; Kirillova, M.V.; Kirillov, A.M. Copper(II) Coordination Polymers Self-Assembled from Aminoalcohols and Pyromellitic Acid: Highly Active Precatalysts for the Mild Water-Promoted Oxidation of Alkanes. *Inorg. Chem.* **2016**, *55*, 125. [CrossRef]
9. Yoshikawa, Y.; Yasui, H. Zinc Complexes Developed as Metallopharmaceutics for Treating Diabetes Mellitus based on the Bio-Medicinal Inorganic Chemistry. *Curr. Top. Med. Chem.* **2012**, *12*, 210. [CrossRef]
10. Muche, S.; Levacheva, I.; Samsonova, O.; Pham, L.; Christou, G.; Bakowsky, U.; Hołyńska, M. A Chiral, Low-Cytotoxic [Ni15]-Wheel Complex. *Inorg. Chem.* **2014**, *53*, 7642. [CrossRef]
11. Vančo, J.; Marek, J.; Travniček, Z.; Račanska, E.; Muselik, J.; Švajlenova, O. Synthesis, structural characterization, antiradical and antidiabetic activities of copper(II) and zinc(II) Schiff base complexes derived from salicylaldehyde and β-alanine. *J. Inorg. Biochem.* **2008**, *102*, 595. [CrossRef] [PubMed]
12. Yin, D.-D.; Jiang, Y.-L.; Shan, L. Synthesis, characterization of diorganotin (IV) schiff base complexes and their in vitro antitumor activity. *Chin. J. Chem.* **2001**, *19*, 1136. [CrossRef]
13. Vanco, J.; Svajlenova, O.; Racanska, E.; Muselik, J.; Valentova, J.; Elem, J. Antiradical activity of different copper(II) Schiff base complexes and their effect on alloxan-induced diabetes. *Med. Biol.* **2004**, *18*, 155.
14. Serna, Z.; De la Pinta, N.; Urtiaga, M.K.; Lezama, L.; Madariaga, G.; Juan, J.M.; Coronado, E.; Cortes, R. Defective Dicubane-like Tetranuclear Nickel(II) Cyanate and Azide Nanoscale Magnets. *Inorg. Chem.* **2010**, *49*, 11541. [CrossRef]
15. Wang, H.; Wan, C.-Q.; Mak, T.C.W. High-nuclearity silver(I) cluster-based coordination polymers assembled with multidentate oligo-α-heteroarylsulfanyl ligands. *Dalton Trans.* **2014**, *43*, 7254. [CrossRef] [PubMed]
16. Chen, C.; Zhang, J.; Li, G.; Shen, P.; Jin, H.; Zhang, N. Two coordination polymers constructed from a multidentate carboxylic acid ligand with a tertiary amine serve as acid–base catalysts for the synthesis of chloropropene carbonate from $CO_2$ under atmospheric pressure. *Dalton Trans.* **2014**, *43*, 13965. [CrossRef] [PubMed]
17. Penney, M.K.; Giang, R.; Burroughs, M.A., Jr.; Klausmeyer, K.K. Structure and luminescence of discrete and polymeric Ag(I) complexes formed by the multidentate pyridylphosphine $(PPh_2CH_2)_2N(3\text{-}CH_2C_5H_4N)$. *Polyhedron* **2015**, *87*, 43. [CrossRef]
18. Landers, A.E.; Phillips, D.J. Alkoxy-bridged complexes of copper(II) and nickel(II) with schiff bases of alcoholamines-including effects of structural distortion on the electronic spectra of Six-coordinate nickel(II) Complexes. *Inorg. Chim. Acta* **1979**, *32*, 53. [CrossRef]
19. Si, S.-F.; Tang, J.-K.; Liao, D.-Z.; Jiang, Z.-H.; Yan, S.-P. Synthesis, structure, and characterization of dicopper(II) complex with a new amidate ligand. *Inorg. Chem. Commun.* **2002**, *5*, 76. [CrossRef]
20. Xie, Y.; Jiang, H.; Chan, A.S.C.; Liu, Q.L.; Xu, X.L.; Du, C.X.; Zhu, Y. Structural and magnetic properties of O-bridged tetranuclear and binuclear Cu(II) complexes. *Inorg. Chim. Acta* **2002**, *333*, 138. [CrossRef]
21. Koikawa, M.; Yamashita, H.; Tokii, T. Crystal structures and magnetic properties of tetranuclear copper(II) complexes of *N*-(2-hydroxymethylphenyl)salicylideneimine with a defective double-cubane core. *Inorg. Chim. Acta* **2004**, *357*, 2635. [CrossRef]
22. Titi, A.; Shiga, T.; Oshio, H.; Touzani, R.; Hammouti, B.; Mouslim, M.; Warad, I. Synthesis of novel Cl2Co4L6 clusterusing 1-hydroxymethyl-3,5-dimethylpyrazole (LH) ligand: Crystal structure, spectral, thermal, Hirschfeld surface analysis and catalytic oxidation evaluation. *J. Mol. Struct.* **2020**, *1199*, 126995. [CrossRef]
23. Titi, A.; Oshio, H.; Touzani, R.; Mouslim, M.; Zarrouk, A.; Hammouti, B.; Al-Zaqri, N.L.; Alsalme, A.; Warad, I. Synthesis and XRD of Novel Ni4(μ3-O)4 Twist Cubane Cluster Using Three NNO Mixed Ligands: Hirshfeld, Spectral, Thermal and Oxidation Properties. *J. Clust. Sci.* **2020**, *26*, 1. [CrossRef]
24. Zienkiewicz, M.; Jabłonska-Wawrzycka, A.; Szlachetko, J.; Kayser, Y.; Stadnicka, K.; Sawka-Dobrowolska, W.; Jezierska, J.; Barszcz, B.; Sá, J. Effective catalytic disproportionation of aqueous H2O2 with di- and mono-nuclear manganese(ii) complexes containing pyridine alcohol ligands. *Dalton Trans.* **2014**, *43*, 8599. [CrossRef]
25. Zienkiewicz, M.; Szlachetko, J.; Lothschütz, C.; Hodorowicz, M.; Wawrzycka, A.; Sá, J.; Barszcz, B. A novel single-site manganese(II) complex of a pyridine derivative as a catalase mimetic for disproportionation of $H_2O_2$ in water. *Dalton Trans.* **2013**, *42*, 7761. [CrossRef]

26. El Kodadi, M.; Malek, F.; Touzani, R.; Ramdani, A. Synthesis of new tripodal ligand 5-(bis(3,5-dimethyl-*1H*-pyrazol-1-ylmethyl)amino)pentan-1-ol, catecholase activities studies of three functional tripodal pyrazolyl N-donor ligands, with different copper (II) salts. *Catal. Commun.* **2008**, *9*, 966. [CrossRef]
27. Kim, E.; Woo, H.Y.; Kim, S.; Lee, H.; Kim, D.; Lee, H. Synthesis and X-ray crystal structure of derivatives from the *N*,*N*-bis(1H-pyrazolyl-1-methyl)aniline(dichloro)Zn(II) complex: Substituent effects on the phenyl ring versus the pyrazole ring. *Polyhedron* **2012**, *42*, 135. [CrossRef]
28. Otero, A.; Fernández-Baeza, J.; Lara-Sánchez, A.; Sánchez-Barba, L.F. Metal complexes with heteroscorpionate ligands based on the bis(pyrazol-1-yl)methane moiety: Catalytic chemistry. *Coord. Chem. Rev.* **2013**, *257*, 1806. [CrossRef]
29. Xue, F.; Zhao, J.; Hor, A.T.S. Cross-coupling of alkyl halides with aryl or alkyl Grignards catalyzed by dinuclear Ni(ii) complexes containing functionalized tripodal amine-pyrazolyl ligands. *Dalton Trans.* **2013**, *42*, 5150. [CrossRef]
30. Han, X.-B.; Li, Y.-G.; Zhang, Z.-M.; Tan, H.-Q.; Lu, Y.; Wang, E.-B. Polyoxometalate-Based Nickel Clusters as Visible Light-Driven Water Oxidation Catalysts. *J. Am. Chem. Soc.* **2015**, *137*, 5486. [CrossRef]
31. Asadi, Z.; Zarei, L.; Golchin, M.; Skorepova, E.; Eigner, V.; Amirghofran, Z. A novel Cu(II) distorted cubane complex containing $Cu_4O_4$ core as the first tetranuclear catalyst for temperature dependent oxidation of 3,5-di-*tert*-butyl catechol and in interaction with DNA & protein (BSA). *Spectrochim. Acta A* **2020**, *227*, 117593.
32. Driessen, W.L. Synthesis of some new pyrazole-containing chelating agents. *Recl. Trav. Chim. Pays-Bas* **1982**, *101*, 441. [CrossRef]
33. Wolff, S.K.; Grimwood, D.J.; McKinnon, J.J.; Jayatilaka, D.; Spackman, M.A. CrystalExplorer2. 1. University of Western Australia. In *Crystal Explorer 2.1*; University of Western Australia: Perth, Australia, 2007.
34. Sheldrick, G.M. A magic triangle for experimental phasing of macromolecules. *Acta Cryst.* **2008**, *64*, 112. [CrossRef] [PubMed]
35. Ng, C.K.; Tam, T.L.D.; Wei, F.; Lub, X.; Wu, J. Anion–π and anion–π-radical interactions in bis(triphenylphosphonium)-naphthalene diimide salts. *Org. Chem. Front.* **2019**, *6*, 110. [CrossRef]
36. Dorn, T.; Janiak, C.; Abu-Shandi, K. Hydrogen-bonding, pi-stacking and Cl-anioninteractions of linear bipyridinium cations with phosphate, chloride and $[CoCl_4]$ 2-anions. *CrystEngComm* **2005**, *7*, 633–641. [CrossRef]
37. Warad, I.; Awwadi, F.F.; Al-Ghani, B.A.; Sawafta, A.; Shivalingegowda, N.; Lokanath, N.K.; Mubarak, M.S.; Hadda, T.B.; Zarrouk, A.; Al-Rimawi, F.; et al. Ultrasound-assisted synthesis of two novel $[CuBr(diamine)_2{\cdot}H_2O]Br$ complexes: Solvatochromism, crystal structure, physicochemical, Hirshfeld surface thermal, DNA/binding, antitumor and antibacterial activities. *Ultrason. Sonochem.* **2018**, *48*, 1. [CrossRef]
38. Warad, I.; Al-Demeri, Y.; Al-Nuri, M.; Shahwan, S.; Abdoh, M.; Naveen, S.; Lokanath, N.K.; Mubarak, M.S.; Hadda, T.B.; Mabkhot, Y.N. Crystal structure, Hirshfeld surface, physicochemical, thermal and DFT studies of ($N_1E$, $N_2E$)-$N_1$,$N_2$-bis((5-bromothiophen-2-yl)methylene)ethane-1,2-diamine $N_2S_2$ ligand and its $[CuBr(N_2S_2)]Br$ complex. *J. Mol. Struct.* **2017**, *1142*, 217. [CrossRef]
39. Saleem, F.A.; Musameh, S.; Sawafta, A.; Brandao, P.; Tavares, C.J.; Ferdov, S.; Barakat, A.; Al Ali, A.; Al-Noaimi, M.; Warad, I. Diethylenetriamine/diamines/copper (II) complexes [Cu(dien)(NN)]Br2: Synthesis, solvatochromism, thermal, electrochemistry, single crystal, Hirshfeld surface analysis and antibacterial activity. *Arab. J. Chem.* **2017**, *10*, 845. [CrossRef]
40. Warad, I.; Khan, A.A.; Al-Resayes, S.I.; Haddad, S.F. Design and structural studies of diimine/$CdX_2$ (X = Cl, I) complexes based on 2,2-dimethyl-1,3-diaminopropane ligand. *J. Mol. Struct.* **2014**, *1062*, 167. [CrossRef]
41. Aouad, M.R.; Messali, M.; Rezki, N.; Al-Zaqri, N.; Warad, I. Single proton intramigration in novel 4-phenyl-3-((4-phenyl-1*H*-1,2,3-triazol-1-yl)methyl)-1*H*-1,2,4-triazole-5(4*H*)-thione: XRD-crystal interactions, physicochemical, thermal, Hirshfeld surface, DFT realization of thiol/thione tautomerism. *J. Molec. Liq.* **2018**, *264*, 621. [CrossRef]
42. Warad, I.; Eftaiha, A.A.F.; Al-Nuri, M.A.; Husein, A.I.; Assal, M.; Abu-Obaid, A.; Al-Zaqri, N.; Hadda, T.B.; Hammouti, B. Metal ions as Antitumor Complexes-Review. *J. Mater. Environ. Sci.* **2013**, *4*, 542.
43. Alkorta, I.; Elguero, J.; Grabowski, S.J. How To Determine Whether Intramolecular H···H Interactions Can Be Classified as Dihydrogen Bonds. *J. Phys. Chem. A* **2008**, *112*, 2721. [CrossRef] [PubMed]
44. Richardson, B.; De Gala, S.; Crabtree, H.; Siegbahn, M. Unconventional Hydrogen Bonds: Intermolecular B-H···H-N Interactions. *J. Am. Chem. Soc.* **1995**, *117*, 12875. [CrossRef]

45. Cramer, J.; Gladfelter, L. Ab Initio Characterization of $[H_3N{\cdot}BH_3]_2$, $[H_3N{\cdot}AlH_3]_2$, and $[H_3N{\cdot}GaH_3]_2$. *Inorg. Chem.* **1997**, *36*, 5358. [CrossRef]
46. Warad, I.; Alkanad, K.; Suleiman, M.; Kumara, K.; Al-Ali, A.; Mohammed, Y.; Lokanath, N.K.; Zarrouk, A. Design, structural, C–H . . . .H–C supramolecular interactions and computational investigations of Cd(N∩N′′)X 2 complexes based on an asymmetrical 1,2-diamine ligand: Physicochemical and thermal analysis. *J. Coord. Chem.* **2019**, *72*, 12. [CrossRef]
47. Thakurta, S.; Pilet, G.; Luneau, D.S. A novel tetra(μ3-phenoxo) bridged copper(II) Schiff base complex containing a $Cu_4O_4$ cubane core: Synthesis, structural aspects and magneto-structural correlations. *Mitra Polyhedron* **2009**, *28*, 819.
48. Tauc, J.; Menth, A.; Optical processes in solids. Non-Cryst, J. *Solids* **1972**, *8*, 569.
49. Aziz, B.; Abdullah, M. Crystalline and amorphous phase identification from the tanδ relaxation peaks and impedance plots in polymer blend electrolytes based on [CS:AgNt]x:PEO(x-1) ($10 \leq x \leq 50$). *Electrochim. Acta* **2018**, *285*, 30. [CrossRef]
50. Kaddouri, Y.; Haddari, H.; Titi, A.; Yousfi, E.B.; Chetouani, A.; El Kodadi, M.; Touzani, R. Catecholase catalytic properties of copper (II) complexes prepared in-situ with heterocyclic ligands: Experimental and DFT study. *Mor. J. Chem.* **2020**, *8*, 184.
51. Titi, A.; Al-Noaimi, M.; Kaddouri, Y.; El Ati, R.; Yousfi, E.B.; El Kodadi, M.; Touzani, R. Study of the catecholase catalytic properties of copper (II) complexes prepared in-situ with monodentate ligands. *Mater. Today Proc.* **2019**, *13*, 1134. [CrossRef]
52. Modak, R.; Sikdar, Y.; Mandal, S.; Goswami, S. Synthesis, Crystal Structures, Magnetic Properties and Catecholase Activity of Double Phenoxido-Bridged Penta-Coordinated Dinuclear Nickel(II) Complexes Derived from Reduced Schiff-Base Ligands: Mechanistic Inference of Catecholase Activity. *Inorg. Chem. Commun.* **2013**, *9*, 26.
53. Indira, S.; Vinoth, G.; Bharathi, M.; Bharathi, S.; Rahiman, A.K.; Bharathi, K.S. Catechol oxidase and phenoxazinone synthase mimicking activities of mononuclear Fe(III) and Co(III) complexes of amino-bis(phenolate)-based mixed ligands: Synthesis, spectral and electrochemical studies. *Inorg. Chim. Acta* **2019**, *495*, 118988. [CrossRef]
54. Mandal, L.; Sasmal, S.; Sparkes, H.A.; Howard, J.A.K.; Mohanta, S. Crystal structure, catecholase activity and ESI-MS of a mixed valence cobalt(III)–cobalt(II) complex derived from a macrocyclic ligand: Identification/proposition of hydrogen bonded metal complex· · · solvent aggregates in ESI-MS. *Inorg. Chim. Acta* **2014**, *412*, 38. [CrossRef]